Hydrol. Earth Syst. Sci. Discuss., 10, 6445–6471, 2013
www.hydrol-earth-syst-sci-discuss.net/10/6445/2013/
doi:10.5194/hessd-10-6445-2013

Hydrology and Earth System Sciences
Discussions

Climate changes of hydrometeorological and hydrological extremes in the Paute basin, Ecuadorean Andes

D. E. Mora[1,2], **L. Campozano**[5], **F. Cisneros**[2], **G. Wyseure**[4], **and P. Willems**[1,3]

[1]KU Leuven, Hydraulics Divison, Kasteelpark Arenberg 40, 3001 Leuven, Belgium
[2]Universidad de Cuenca, Programa para el Manejo del Agua y del Suelo PROMAS, Av. 12 de abril, Cuenca, Ecuador
[3]Vrije Universiteit Brussel, Department of Hydrology & Hydraulic Engineering, Pleinlaan 2, 1050 Brussels, Belgium
[4]Katholieke Universiteit Leuven, Soil and Water Management Divison, Celestijnenlaan 200E, 3001 Leuven, Belgium
[5]Universidad de Cuenca, Av. 12 de abril, Cuenca, Ecuador

Received: 30 April 2013 – Accepted: 8 May 2013 – Published: 24 May 2013

Correspondence to: D. E. Mora (diego.nora@ucuenca.edu.ec)

Published by Copernicus Publications on behalf of the European Geosciences Union.

Abstract

Investigation was made on the climate change signal for hydrometeorological and hydrological variables for the Paute River basin, in southern Ecuador Andes, making use of an adjusted quantile perturbation approach for climate downscaling, and the impact of climate change on runoff for two nested catchments within the basin. The analysis was done making use of long daily series of seven representative rainfall and temperature sites along the study area and considering climate change signals of global and regional climate models for IPCC SRES scenarios A1B, A2 and B1. The determination of runoff was carried out using a lumped conceptual rainfall-runoff model.

The study found that the range of changes in temperature is despicably lower that the range of changes in rainfall. However, changes differ from site to site, showing that more significant changes in temperature are observed at higher elevation sites. For rainfall, high differences in rainfall change are found and strongly related to the rainfall regime. Higher changes are detected for sites located in regions with bimodal rainfall regime. In addition, higher changes are observed on higher temporal resolutions. The runoff changes are strongly related to the changes in rainfall peaks, more than with the changes in temperature; also showing strong spatial differences over the Andean region considered.

1 Introduction

The impact of climate change on hydrological systems is receiving higher attention during the last decades due to its consequences on water resources, especially related to droughts and floods (Nijssen et al., 2001; Hirabayashi et al., 2008; Dirmeyer et al., 2012). Changes in rainfall are strongly related with changes in runoff and therefore with water availability. Changes in temperature, humidity, atmospheric pressure are related with changes in evapotranspiration, which is also an important input of the hydrological system. In addition, rainfall intensity is a primary weathering agent for rocks and soils

HESSD
10, 6445–6471, 2013

increasing the transport of sediments and dissolved solids to water bodies. Furthermore, hydrological processes at the land surface influence the natural environment at a range of spatial and temporal scales through their impacts on biological activity and water chemistry (Beldring et al., 2008). This is also the case for the Paute river basin in Ecuador, where future climate change might severely impact hydrological and ecological conditions. Especially the water availability is a concern (Ontaneda et al., 2002), due to changes in temperature and humidity and high variability in rainfall extreme events (Parry et al., 2007).

A common methodology to quantify climate change signals makes use of General Circulation Model or Global Climate Model (GCM) results. These results might, however, be too coarse to provide regional and local details, and should not be used directly for hydrological modeling, especially for regions with a high spatial and temporal variability in climate variables. This is the case of the Paute river basin in the Tropical Andes in south Ecuador (Celleri et al., 2007; Mora and Willems, 2012). One solution is the use of Regional Climate Model (RCM) results, which provides finer scale information. However, Buytaert et al. (2010) state that for some tropical regions and scales of aggregation, RCMs may produce inappropriate results compared with GCMs, especially for precipitation.

To solve this problem, different statistical downscaling techniques, with different strengths and weaknesses (Fowler et al., 2007) were developed in order to obtain a higher spatial resolution (Giorgi et al., 2001; Hewitson and Crane, 1996). The application of these downscaling techniques to climate variables as rainfall and temperature may account for the mesoscale hydro-climatologic processes for areas of complex topography. Within them, the delta change or perturbation techniques are developed to translate large-scales GCM/RCM outputs onto a finer resolution based on change factors (Prudhomme et al., 2002; Willems et al., 2012). The change factors consider the differences between control and future GCM/RCM simulations and are applied to observed series.

HESSD
10, 6445–6471, 2013

Taking this state-of-the-art into account, this paper aims to compare different projections of climate models for the Paute river basin after the application of an adjusted change factor based statistical downscaling method, the Quantile Perturbation Approach (QPA) and the effect in flows for two catchments in the basin. The application of this method implies: (i) the use of a perturbation factor (PF) dependent of the rainfall intensity exceedance probability; (ii) the consideration of a PF on the number of wet and dry days; (iii) the application of a relative PF combined with an absolute change, and (iv) the placement in time of new wet-dry days according to volume and length of wet-dry spells.

Following sections describe the study area, the data, the adjusted QPA and the evaluation of the approach. This is followed by a section that presents and discusses the climate change impact results. The final section summarizes this study with some concluding remarks.

2 Methodology

2.1 Study area

The basin of the river Paute is located in the Inter-Andean Depression separating the Western and Real Cordillera in the south of Ecuador (Coltorti and Ollier, 2000). With an area of 5066 km^2 and elevation range from 1840 to 4680 m a.s.l. the basin has a vital hydropower plant complex at its downstream end. The upper part of the basin is located only 17 km from the Pacific coastal plains and 62 km from the Pacific coast line at its western point. The downstream part of the basin ends in the interspersed region between the Andes and the Amazon (Fig. 1). For the discharge analysis, two subcatchments within the Paute river basin are analyzed. The catchment of Tomebamba in Monay (To Mo) is located in the western headwaters of the Paute river basin. It has an extension of 1265 km^2 and an elevation range between 2500 and 4680 m a.s.l. Within this catchment the city of Cuenca is located with nearly 400 000 inhabitants

HESSD
10, 6445–6471, 2013

(third on national importance). The catchments consist mainly of páramo and native forest, agriculture and urban areas. Within the catchment of To Mo, the subcatchment of Matadero in Sayausi (Ma Sa) is located with an area of 300 km^2

2.2 Database

The Paute river basin is one of the most monitored basins in Ecuador. It has rainfall and temperature observation records since 1963 due to its importance in hydropower energy production. For this research, 7 sites located in different rainfall regime regions and at varying elevations were selected. The available data series start near 1962–1964 and continue till 1992–1993 with daily series for rainfall and monthly series for mean temperature. The names and characteristics of these sites are shown in Table 1. The available GCM-RCM control and scenario simulations covering Ecuador, which were considered in this study, are shown in Table 1. The control runs are available with daily simulation results for the historical period 1961–1990 and the future scenarios simulation results for 2045–2065. The simulated future greenhouse gas emissions were based on the IPCC Special Report on Emission Scenario (SRES) for the A1B, A2 and B1 scenarios (Nakicenovic et al., 2000; Solomon et al., 2007).

2.3 Perturbation or delta approach

The perturbation approach is the most common method to transfer the signal of climate change from a climate system level represented by climate models to the hydrological system level represented by hydrological models (Middelkoop et al., 2001; Andréasson et al., 2004; Nguyen et al., 2007; Olsson et al., 2012; Willems et al., 2012). This method regroups the advantages of dynamical and statistical downscaling approaches extracting the climate signals from GCMs and RCMs, which are improving continuously in time and space, and makes use of observed climate series properties as a baseline on which the climate change signals are applied.

HESSD
10, 6445–6471, 2013

This method is applied to the most relevant climate variables in hydrology, notably rainfall and ETo. In it most simple form, monthly perturbation factors, Eqs. (1) and (2), are determined and applied to the input series of hydrological models:

$$T_{\mathrm{F,daily}} = T_{\mathrm{ob,daily}} + \left(T_{\mathrm{CMF,monthly}} - T_{\mathrm{CM20th,monthly}}\right) \quad (1)$$

$$P_{\mathrm{F,daily}} = P_{\mathrm{ob,daily}} \cdot \left(\frac{P_{\mathrm{CMF,monthly}}}{P_{\mathrm{CM20th,monthly}}}\right) \quad (2)$$

where T_{ob} and P_{ob} are the observed temperature and rainfall values in the series, T_{CM20th} and P_{CM20th} the 20th century climate model control run results, T_{CMF} and P_{CMF} the projected future climate model results and T_{F} and P_{F} the projected future results after perturbation.

However, some of the disadvantages of this method include the assumption of no shift in the shape and type of changes. Extremes are indeed modified by the same factor as the other events. In addition, the assumption of no change in the number or the frequency of events is another disadvantage (Harrold and Jones, 2003).

2.4 Adjustments to the perturbation approach

The adjusted perturbation approach considers a climate change signal on both the number of wet or dry days and on the rainfall intensity. The change in the rainfall intensity is calculated in a quantile-based way, making use of a quantile mapping technique (Nguyen et al., 2008; Ntegeka and Willems, 2008; Willems and Vrac, 2011) hence with the PF depending on the exceedance probability threshold. The method is applied with a relative PF or an absolute shift in the rainfall intensity, depending on whether relative or absolute change is applied.

The change in wet day frequency is calculated as the ratio of the number of wet days for the scenario period (2045–2065) over the number of wet days for the control

HESSD
10, 6445–6471, 2013

period (1961–1990) considering that a wet day is any day with rainfall depth above a certain threshold *wd_th*. The PF on the wet day frequency (PF_{wf}) is > 1 when the scenario series have more wet days than the control series and PF_{wf} is < 1 when dry days should be added (or wet days should be removed) from the observed series.

Once the PF_{wf} is obtained, the PF on the wet day rainfall intensity (PF_{ri}) is determined in a quantile based way by comparing ranked daily extremes from the control period vs. the scenario period. Instead of using a unique PF for all events, the rainfall intensity PF is obtained dependent on the empirical exceedance probability of the intensity. However, the application of a relative intensity PF on observed values close to zero will produce signal changes near to zero even if the PF is high, or vice-versa, small absolute changes between scenario and control values might lead to excessive PF when the control value is close to zero. Therefore the inclusion of an absolute change applied to rainfall intensities α under a threshold exceedance probability is considered in the adapted methodology. For high rainfall intensities corresponding to exceedance probabilities below $p(\alpha)$, a relative rainfall intensity PF is applied. For rainfall intensities corresponding to exceedance probabilities above $p(\alpha)$ the rainfall intensity change is derived by calculation of a weighted average of the relative and absolute rainfall intensity changes. The weighting factor varies linearly between $p(\alpha)$ and $p(0)$, where $p(0)$ is the exceedance probability of the ranked rainfall intensities equal to the wet day threshold on the observed series (see Fig. 3).

In case $PF_{wf} > 1$ wet days need to be added to the observed series to obtain perturbed series. The intensities of these days are taken from the absolute change in rainfall intensity corresponding to exceedance probabilities above $p(0)$.

For the addition of the different wet/dry days, the wet/dry spells are first identified in the observed series and ranked per month according to rainfall volume and rainfall duration of the different spells. In case new days need to be added, the first wet day will be add at the end of the highest rainfall volume/duration wet event. A second day will be added at the end of the second highest event and so on. In the case that a dry day is added, a wet day rainfall intensity will be changed to zero at the end of the lowest

HESSD
10, 6445–6471, 2013

rainfall volume event and at the end of the longest duration dry event. In case that the number of new wet or dry days is higher than the number of wet or dry spells, the addition of new days will start again in the ranked events.

This method solves the above mentioned problem related to the application of a relative PF to low rainfall intensities and allows to determine the rainfall intensity values of the additional wet days.

2.5 Rainfall-runoff model

The downscaled future series of rainfall and evapotranspiration were used for the study of the climate change impact on river discharges based on a calibrated lumped conceptual model with emphasis on the peak flows. The model has been implemented using the generalized lumped conceptual and parsimonious model structure-identification and calibration (VHM) approach of Willems (2000, 2013), previously also applied for hydrological climate change or variability impact analysis by Taye et al. (2011), Liu et al. (2011), Van Steenbergen and Willems (2012) and Taye and Willems (2013). VHM is a a data-based approach for lumped conceptual model structure identification and calibration. Only the key aspects are presented here. The model summarizes in a few parameters the combined effect of the different hydrological processes for each catchment, which starts from a generalized model structure framework that is adjusted in a case-specific parsimonious optimal way. Using separate analysis of recession constants, routing submodels and runoff-subflow separation processes, a data-based and step-wise transparent model-structure identification and calibration is obtained.

The equations of Penman–Monteith (Penman, 1948; Monteith, 1965) were used to estimate future evapotranspiration (ETo) series considering the future temperature series previously described. For each cathment, future rainfall and ETo input series were estimated from the results of the downscaled climate model runs at each site and interpolating according to the inverse distance weighted method.

Calibration of the rainfall-runoff model was done making use of observed series for a period of three years and evaluated by the Nash–Sutcliffe (NS) model efficiency

HESSD
10, 6445–6471, 2013

(Nash and Sutcliffe, 1970) and by the peak flow mean squared error (PFE) based on total runoff flows (simulated versus observed flows). Different calibration methodologies were tested: the step-wise model calibration (Willems, 2000), the step-wise model optimization and the overal model optimization (Willems et al., 2013) in order to obtain optimal statistics. The numerical optimization techniques are based on the SCEM-UA search algoritm (Vrugt et al., 2003). Daily time step was considered as for the rainfall and temperature inputs.

2.6 Impact indicators

In order to evaluate the impact of the different climate scenario projections on temperature, rainfall and discharge, statistical measures are used for the difference between the observed series and the perturbed observed series of rainfall and temperature for different scenarios at the mentioned sites in the study region. The impact indicators considered are the mean relative change and the root mean squared relative change, shown in Eqs. (3) and (4) respectively, for monthly and daily series. The mean relative change provides information on the mean change among the different models and/or observed series and/or scenarios, whereas the root mean squared relative change reflects the variability in the changes. In addition, the arithmetic mean (Av), minimum (Min) and maximum (Max) on daily rainfall and flow were also considered, for both the projected and observed series.

$$M_{\mathrm{p,q}} = \frac{1}{n}\sum_{j=i}^{n}\left(\frac{(X_{\mathrm{p}})_n - (Y_{\mathrm{q}})_n}{(Y_{\mathrm{q}})_j}\right) \times 100 \quad \text{for } p = 1 \text{ to } m \text{ and } q = 1 \text{ to } s \tag{3}$$

$$\mathrm{RMS}_{\mathrm{p,q}} = \sqrt{\frac{1}{n}\sum_{j=i}^{n}\left(\frac{(X_{\mathrm{p}})_n - (Y_{\mathrm{q}})_n}{(Y_{\mathrm{q}})_j}\right)^2} \times 100 \quad \text{for } p = 1 \text{ to } m \text{ and } q = 1 \text{ to } s \tag{4}$$

HESSD
10, 6445–6471, 2013

where M and RMS are the mean relative change and the root mean square relative change respectively; $(X_p)_j$ and $(Y_q)_j$ are the perturbed observed and observed series respectively; m and s are the number of climate model control-scenario run combinations considered and number of observed sites respectively, and n the number of year, month or day records.

3 Results

The adjusted perturbation approach was applied to observed daily rainfall series and monthly mean temperature series for the Paute River basin in areas with different rainfall regimes and at different elevations. The climate change signals were studied for the ensemble of all GCM control – scenario run combinations. The impact results are explained on Table 2, excluding outliers. The ranges of change were compared between sites and scenarios.

Taking the daily rainfall series at site M067 and the scenario A1B as example, results of the different criteria can be seen in Fig. 4a–d. For this specific case, rainfall shows an increase for most of the GCM runs. The monthly and yearly cumulative rainfall mean changes M are 15 and 13 % and the RMS are 34 and 15 %, respectively, bringing a higher variability in change in monthly series. When daily rainfalls are analyzed, this site shows that the ensemble results gave average increases of 40 and 20 % for the maxima and average daily rainfalls respectively. The change on extremes is higher than the change on average rainfalls, seen on Fig. 4d. However, three GCM runs gfdl_cm2_0_run1, giss_model_e_r_run1 and ipsl_cm4_run1 are considered as outliers for this site. The first two model runs show very high extreme daily events, and the other one shows a high decrease of daily, monthly and yearly cumulative rainfall. As expected, the maximum daily and monthly rainfall depths show a wider range of uncertainty in the future predictions than the average rainfalls.

The same analysis was performed for rainfall, temperature and discharge changes after scenarios A2 and B1 for all sites. Results are summarized in Table 2.

HESSD
10, 6445–6471, 2013

For the mean monthly temperature, results for all sites show an average increase between 8 and 23 % (between 1.2 and 3.0 °C). The changes are higher for site M141 than other sites and the lower change rate is found at site M139. Additionally, higher changes are estimated with scenario A1B than any other scenario. Maximum and minimum average temperatures change at different rates. For all sites, the minimum average temperature increases with higher rates than the average and maximum temperatures, meaning that low temperatures will rise higher than high temperatures. However, the uncertainty in the change of minimum temperatures is also higher, where some GCMs even show temperature decreasing rates. When changes are related to elevation, changes are higher at higher elevation.

For rainfall, results indicate an average increase between 12 and 27 % (between 0.5 to 1.3 mm) for daily rainfall; between 7.5 and 18 % (between 8.0 and 18 mm) for monthly rainfall; between 15 and 58 % (between 12 and 34 mm) for daily rainfall maxima, and between 9.5 and 52 % (between 36 and 140 mm) for monthly rainfall maxima. The average increase in rainfall is higher at sites M067 and M424, meanwhile site M141 shows the lowest increase rate. In addition, a higher increase is visible for scenario A2 than the other scenarios in all cases, with few exceptions. Changes in the daily rainfall maxima are higher than the changes in the mean daily rainfall intensity, showing that higher changes are present at high rainfall intensities (see Table 2).

To summarize these results, a map of the changes on the average daily rainfall and average monthly mean temperature is shown in Fig. 5. The higher heterogeneity of the region is confirmed in this study, where higher elevation sites show a higher increase in temperature. For rainfall, this heterogeneity is even stronger. Dependent on the rainfall regime, increases are higher or lower. The average rate of change for sites located in the bi-modal rainfall regime is nearly 20 % while this change is 14 % for the region UM1. The site M141, located in the western páramo region, named as bi-modal 2, shows a lower change rate than other bi-modal sites. This might be due to the fact that the site is located on the western region of the basin and might be affected by Pacific drivers considered in the climate models. However, a completely different distribution

HESSD
10, 6445–6471, 2013

might be seen if maxima would be shown. In this case, as seen in Table 2, the higher change rates are located along the entire basin independent of the regime.

The rainfall-runoff model impacts differ depending on the parameter set considered, which means depending on the model calibration method. Table 3 show the model performance evaluation results of the different calibration techniques. The table shows that for both catchments, the best model is obtained with the use of the step-wise model calibration. In Willems et al. (2013) it is shown that numerical optimization can achieve better overall results, but that it does not guarantee accurate submodels. Changes in discharges were analyzed with the same method as done for rainfall and temperature, but after a conversion of discharges in unitary runoffs, this is relative to its area. In both catchments, the average runoff increases with similar rates. The mean change rate for To Mo is in the order of 8 % while it is 10 % for Ma Sa, showing no apparent correspondence with the change rates on rainfall and temperature. The RMS of the change is nearly similar for both: 35 % for To Mo and 30 % for Ma Sa. However, when extremes are analyzed, the To Mo increases are higher than for Ma Sa (see Fig. 6). In the case of scenario A2, the change on the runoff maxima is 64 % for To Mo while it is only 41 % for Ma Sa. This difference might be due to the fact that To Mo includes higher areas belonging to the BM1 rainfall regime, where a higher rainfall increase was found. In addition, Ma Sa involves areas with higher elevation where temperature increases are higher and the rate of change in rainfall, both average and extremes, is lower. However, higher uncertainty is also found for the extremes. As for rainfall, the higher changes for runoff are also present for scenario A2. This point towards the conclusion that rainfall changes have more weight, in contrast to temperature changes in their influence to changes in runoff.

HESSD
10, 6445–6471, 2013

4 Conclusions

The study brings new knowledge about the behaviour of climate change in a Tropical Andean basin related to the high heterogeneity of the region. This knowledge might be of high support to determine climate change impacts on water resources.

It is concluded from the results that the range of changes in temperature is despicably lower that the range of changes in rainfall. However, the changes strongly differ from site to site. More significant changes in temperature are observed in sites with higher elevation, whereas sites that are allocated in lower elevations show a lower increase. This finding is similar to other previous research studies (Francou et al., 2003; Bradley et al., 2006; Urrutia and Vuille, 2009; Mora and Willems, 2012). However, the number of sites available for this type of research remains limited for the Andean Region.

It is furthermore noticed from our results that the highest monthly temperature values are experimenting lower changes than the average ones and, opposite, the minimum average temperatures meet higher changes. This finding disagrees with the idea that warmest months will become warmer than average. Another insight is that for this region, scenario A1B brings the highest temperature increase. This differs from the global results in which the scenario A2 on average leads to highest temperatures.

The range of changes in rainfall is slightly higher than the changes in temperature for both monthly and yearly scales. However, values of RMS indicate that the variability of the changes is higher at the monthly scale. When yearly, monthly and daily rainfall changes are compared, the dependency of the changes on temporal scale concludes that higher changes are observed for higher temporal resolutions. This conclusion highlights the importance of the analysis making use of high temporal resolution series. Another insight of this study is that higher changes are found in sites located in areas with bimodal rainfall regimes, with strongest changes in the BM1 regime region. This shows that the percentage of change depends on the rainfall regime.

The runoff changes are related with the changes of rainfall peaks stronger than with the temperature changes. However, this conclusion should be taken with care,

HESSD
10, 6445–6471, 2013

as climate change might influence other hydrological parameters that are not taken into account in this study. This is the case for the soil properties of the páramo tropical alpine, which involves a high water retention capacity that is highly dependent on cold temperatures (Buytaert et al., 2011).

As relations are founded between the change signal of temperature and elevation, and changes in rainfall are related with the rainfall region, one has to be cautious when extrapolating the change signals at the current sites based on elevation to other locations in the different rainfall regime regions. The climate change impacts assessed in this study for temperature, rainfall and runoff might bring consequences to the hydrological processes and related water management needs; hence will need further investigation.

Acknowledgements. The research was feasible thanks to a grant of the Selective Bilateral Agreement of the KU Leuven, Belgium, and its cooperation with the Universidad de Cuenca, Ecuador. The research was made within the frame of the VLIR-IUC project Integrated Water Quality Management. Special thanks to the staff of the Hydraulics Division of KU Leuven and to PROMAS-U. Cuenca for the support in research activities and data feasibility. Last but not least, many thanks to Rolando Celleri for his insights and support in the VHM model.

References

Andréasson, J., Bergström, S., Carlsson, B., Graham, L. P., Lindström, G.: Hydrological change – climate change impact simulations for Sweden, AMBIO, 33, 228–234, 2004.

Beldring, S., Engen-Skaugen, T., Førland, E. J., and Roald, L. A.: Climate change impacts on hydrological processes in Norway based on two methods for transferring regional climate model results to meteorological station sites, Tellus A, 60, 439–450, 2008.

Bradley, R. S., Vuille, M., Diaz, H. F., and Vergara, W.: Threats to water supplies in the tropical Andes, Science, 312, 1755–1756, 2006.

Buytaert, W., Vuille, M., Dewulf, A., Urrutia, R., Karmalkar, A., and Célleri, R.: Uncertainties in climate change projections and regional downscaling in the tropical Andes: implications for

HESSD

10, 6445–6471, 2013

water resources management, Hydrol. Earth Syst. Sci., 14, 1247–1258, doi:10.5194/hess-14-1247-2010, 2010.
Buytaert, W., Cuesta-Camacho, F., and Tobón, C.: Potential impacts of climate change on the environmental services of humid tropical alpine regions, Global Ecol. Biogeogr., 20, 19–33, 2011.
Celleri, R., Willems, P., Buytaert, W., and Feyen, J.: Space–time rainfall variability in the Paute basin, Ecuadorian Andes, Hydrol. Process., 21, 3316–3327, 2007.
Coltorti, M. and Ollier, C.: Geomorphic and tectonic evolution of the Ecuadorian Andes, Geomorphology, 32, 1–19, 2000.
Dirmeyer, P. A., Cash, B. A., Kinter, J. L., Stan, C., Jung, T., Marx, L., Towers, P., Wedi, N., Adams, J. M., Altshuler, E. L., Huang, B., Jin, E. K., and Manganello, J.: Evidence for enhanced land – atmosphere feedback in a warming climate, J. Hydrometeorol., 13, 981–995, 2012.
Fowler, H. J., Blenkinsop, S., and Tebaldi, C.: Linking climate change modelling to impacts studies: recent advances in downscaling techniques for hydrological modelling, Int. J. Climatol., 27, 1547–1578, 2007.
Francou, B., Vuille, M., Wagnon, P., Mendoza, J., and Sicart, J.-E.: Tropical climate change recorded by a glacier in the central Andes during the last decades of the twentieth century: Chacaltaya, Bolivia, 16° S, J. Geophys. Res., 108, 4154, doi:10.1029/2002JD002959, 2003.
Giorgi, F., Christensen, J., Hulme, M., von Storch, H., Whetton, P., Jones, R., Mearns, L., Fu, C., Arritt, R., Bates, B., Benestad, R., Boer, G., Buishand, A., Castro, M., Chen, D., Cramer, W., Crane, R., Crossly, J., Dehn, M., Dethloff, K., Dippner, J., Emori, S., Francisco, R., Fyfe, J., Gerstengarbe, F., Gutowski, W., Gyalistras, D., Hanssen-Bauer, I., Hantel, M., Hassell, D., Heimann, D., Jack, C., Jacobeit, J., Kato, H., Katz, R., Kauker, F., Knutson, T., Lal, M., Landsea, C., Laprise, R., Leung, L., Lynch, A., May, W., McGregor, J., Miller, N., Murphy, J., Ribalaygua, J., Rinke, A., Rummukainen, M., Semazzi, F., Walsh, K., Werner, P., Widmann, M., Wilby, R., Wild, M., and Xue, Y.: Regional Climate Information – Evaluation and Projections, in: Climate Change: The Scientific Basis, Contribution of Working Group to the Third Assessment Report of the Intergouvernmental Panel on Climate Change, edited by: Houghton, J. T., Ding, Y., Griggs, D. J., Noguer, M., Van der Linden, P. J., Dai, X., Maskell, K., and Johnson, C. A., Cambridge University Press, Cambridge, UK and New York, US, available at: http://epic.awi.de/4973/ (last access: 26 October 2012), 2001.

HESSD
10, 6445–6471, 2013

Harrold, T. I. and Jones, R.: Downscaling of GCM rainfall: a refinement of the perturbation method, in: EGS-AGU-EUG Joint Assembly, presented at the EGS-AGU-EUG Joint Assembly, 6–11 April 2003, Nice, France, 1338, 2003.
Hewitson, B. and Crane, R.: Climate downscaling: techniques and application, Clim. Res., 07, 85–95, 1996.
Hirabayashi, Y., Kanae, S., Emori, S., Oki, T., and Kimoto, M.: Global projections of changing risks of floods and droughts in a changing climate, Hydrolog. Sci. J., 53, 754–772, 2008.
Liu, T., Willems, P., Pan, X. L., Bao, An. M., Chen, X., Veroustraete, F., and Dong, Q. H.: Climate change impact on water resource extremes in a headwater region of the Tarim basin in China, Hydrol. Earth Syst. Sci., 15, 3511–3527, doi:10.5194/hess-15-3511-2011, 2011.
Middelkoop, H., Daamen, K., Gellens, D., Grabs, W., Kwadijk, J. C. J., Lang, H., Parmet, B. W. A. H., Schädler, B., Schulla, J., and Wilke, K.: Impact of climate change on hydrological regimes and water resources management in the Rhine Basin, Climatic Change, 49, 105–128, 2001.
Monteith, J.: Evaporation and environment, presented at the Symp. Soc. Exp. Biol., Swansea, Cambridge University Press, 1965.
Mora, D. and Willems, P.: Decadal oscillations in rainfall and air temperature in the Paute River Basin – Southern Andes of Ecuador, Theor. Appl. Climatol., 108, 267–282, 2012.
Nakicenovic, N., Alcamo, J., Davis, G., de Vries, B., Fenhann, J., Gaffin, S., Gregory, K., Grubler, A., Jung, T. Y., Kram, T., La Rovere, E. L., Michaelis, L., Mori, S., Morita, T., Pepper, W., Pitcher, H. M., Price, L., Riahi, K., Roehrl, A., Rogner, H.-H., Sankovski, A., Schlesinger, M., Shukla, P., Smith, S. J., Swart, R., van Rooijen, S., Victor, N., and Dadi, Z.: Special Report on Emissions Scenarios: A Special Report of Working Group III of the Intergovernmental Panel on Climate Change, No. PNNL-SA-39650, Pacific Northwest National Laboratory, Richland, WA, USA, Environmental Molecular Sciences Laboratory, USA, Cambridge University Press, New York, USA, 2000.
Nash, J. E. and Sutcliffe, J. V.: River flow forecasting through conceptual models part I – a discussion of principles, J. Hydrol., 10, 282–290, 1970.
Nguyen, V.-T.-V., Desramaut, N., and Nguyen, T.-D.: Estimation of urban design storms in consideration of GCM-based climate change scenarios, water and urban development paradigms: towards an integration of engineering, Design Manage. Approach., Leuven, Belgium, 347–356, 2008.

HESSD
10, 6445–6471, 2013

Nguyen, V.-T.-V., Nguyen, T.-D., and Cung, A.: A statistical approach to downscaling of sub-daily extreme rainfall processes for climate-related impact studies in urban areas, presented at the Sustainable and Safe Water Supplies, International Symposium Hong Kong, China, edited by: International Water Association, 183–192, 2007.

Nijssen, B., O'Donnell, G., Hamlet, A., and Lettenmaier, D.: Hydrologic sensitivity of global rivers to climate change, Climatic Change, 50, 143–175, 2001.

Ntegeka, V. and Willems, P.: Trends and multidecadal oscillations in rainfall extremes, based on a more than, 100 yr time series of, 10 min rainfall intensities at Uccle, Belgium, Water Resour. Res., 44, W07402, doi:10.1029/2007WR006471, 2008.

Olsson, J., Willén, U., and Kawamura, A.: Downscaling extreme short-term regional climate model precipitation for urban hydrological applications, Hydrol. Res., 43, 625–630, 2012.

Ontaneda, G., Garcia, G., and Arteaga, A.: Evidencias del cambio climdtico en Ecuador, Proyecto ECU/99/G31 Cambio Climatico, Fase, 2. Comite Nacional sobre el Clima GEF-PNUD, Ministerio del Ambiente, Quito, Ecuador, 2002.

Parry, M. L., Canziani, O. F., Palutikof, J. P., van der Linden, P. J., and Hanson, C. E.: Contribution of Working Group II to the Fourth Assessment Report of the Intergovernmental Panel on Climate Change, Cambridge, UK, p. 976, 2007.

Penman, H. L.: Natural evaporation from open water, bare soil and grass, P. Roy. Soc. Lond., 193, 120–145, 1948.

Prudhomme, C., Reynard, N., and Crooks, S.: Downscaling of global climate models for flood frequency analysis: where are we now?, Hydrol. Process., 16, 1137–1150, 2002.

Solomon, S., Qin, D., Manning, M., Chen, Z., Marquis, M., Averyt, K., Tignor, M., and Miller, H.: IPCC Fourth Assessment Report: Climate Change, 2007, The Intergovernmental Panel on Climate Change, Cambridge University Press, Cambridge, p. 996, 2007.

Taye, M. T. and Willems, P.: Identifying sources of temporal variability in hydrological extremes of the upper Blue Nile basin, J. Hydrol., in revision, 2013.

Taye, M. T., Ntegeka, V., Ogiramoi, N., and Willems, P.: Assessment of climate change impact on hydrological extremes in two source regions of the Nile River Basin, Hydrol. Earth Sys. Sci., 15, 209–222, 2011.

Urrutia, R. and Vuille, M.: Climate change projections for the tropical Andes using a regional climate model: temperature and precipitation simulations for the end of the 21st century, J. Geophys. Res., 114, D02108, doi:10.1029/2008JD011021, 2009.

HESSD
10, 6445–6471, 2013

Van Steenbergen, N. and Willems, P.: Method for testing the accuracy of rainfall-runoff models in predicting peak flow changes due to rainfall changes in a climate changing context, J. Hydrol., 414–415, 425–434, 2012.

Vrugt, J. A., Gupta, H. V., Bouten, W., and Sorooshian, S.: A Shuffled Complex Evolution Metropolis algorithm for optimization and uncertainty assessment of hydrologic model parameters, Water Resour. Res., 39, 1201, doi:10.1029/2002WR001642, 2003.

Willems, P.: Probabilistic immission modelling of receiving surface waters, PhD Thesis, KU Leuven, Leuven, Belgium, 2000.

Willems, P. and Vrac, M.: Statistical precipitation downscaling for small-scale hydrological impact investigations of climate change, J. Hydrol., 402, 193–205, 2011.

Willems, P., Olsson, J., and Arnbjerg-Nielsen, K.: Impacts of Climate Change on Rainfall Extremes and Urban Drainage Systems, IWA Publishing, London, UK, 239 pp., 2012.

Willems, P., Mora, D. E., Vansteenkiste, T., Taye, M. T., and Van Steenbergen, N.: Parsimonious rainfall-runoff model construction supported by time series processing and validation of hydrological extremes, J. Hydrol., in revision, 2013.

HESSD
10, 6445–6471, 2013

Table 1. GCM/RCM runs for the Ecuadorian region (top), and observed rainfall/temperature sites (bottom).

Model – Run	Center	Country
1. cccr_bcm2_0	Bjerknes Centre for Climate Research	Norway
2. cccma_cgcm3_1	Canadian Centre for Climate Modelling and Analysis	Canada
3. cccma_cgcm3_1_t63		
4. crm_cm3		
5. csiro_mk3_0	Australia's Commonwealth Scientific and Industrial Research Organization	Australia
6. csiro_mk3_5		
7. gfdl_cm2_0	Geophysical Fluid Dynamics Laboratory	USA
8. gfdl_cm2_1		
9. giss_aom	Goddard Institute for Space Studies	USA
10. giss_model_e_r		
11. iap_fgoals1_0_g	Institute of Atmospheric Physics	China
12. ingv_echam4	National Institute of Geophysics and Volcanology	Italy
13. inmcm3_0	Institute for Numerical Mathematics	Russia
14. ipsl_cm4	Institute Pierre Simon Laplace	France
15. miroc3_2_hires	Meteorological Research Institute, Japan	Japan
16. miroc3_2_medres		
17. miub_echo_g	Meteorological Institute, University of Bonn	Germany
18. mpi_echam5	Max-Planck Institute for Meteorology	Germany
19. mri_cgcm2_3_2a	National Institute for Environmental Studies	Japan
20. ncar_ccsm3_0	National Centre for Atmospheric Research	USA
21. ncar_pcm1		
22. Precis Hadley	Hadley Center	UK
23. Precis Echam	Hadley Center – Max-Planck Institute for Meteorology	UK – Germany

Site	Name	Elevation	Region
M410	Rio Mazar-Rivera	2600	UM1
M217	Penas Coloradas	2000	UM2
M139	Gualaceo	2360	BM1
M067	Cuenca Aeropuerto	2516	BM1
M424	Sigsig INAMHI	2600	BM2
M141	El Labrado	3260	BM2
M541	Cochapamba – Quingeo	2760	BM1

HESSD
10, 6445–6471, 2013

Table 2. Results of the impact indicator for rainfall, temperature and runoff changes for the different sites and scenarios. Values indicate an average of the ensemble GCM/RCM runs.

SC	Site	Temp change [%]						Rainfall change [%]								
		Monthly					Yearly	Daily			Monthly				Yearly	
		Max	Min	Av	RMS	Mean	RMS	Mean	Max	Av	Max	Av	RMS	Mean	RMS	Mean
A1B	M067	12.4	18.3	13.0	14.1	13.5	13.5	13.5	39.9	19.8	26.4	12.3	34.0	15.1	14.5	12.8
A2	M067	11.1	16.8	11.8	13.2	12.5	12.6	12.5	57.4	26.8	51.7	17.7	35.3	20.6	15.5	18.4
B1	M067	10.5	12.5	9.1	16.3	14.9	3.8	3.7	40.1	19.3	28.2	11.9	25.1	14.1	10.8	12.4
A1B	M139	9.8	12.7	11.3	12.3	11.8	11.8	11.8	23.3	21.3	23.6	13.3	35.2	16.0	14.9	13.7
A2	M139	9.6	12.1	11.2	12.6	12.0	12.1	12.0	30.5	24.2	27.2	17.0	40.5	20.1	19.0	17.8
B1	M139	7.0	9.4	8.2	16.7	16.2	1.5	1.5	22.3	17.1	16.4	10.6	27.4	13.0	11.8	11.1
A1B	M141	19.4	34.0	22.4	25.2	24.2	24.4	24.2	17.0	16.1	11.8	10.0	26.1	11.9	10.1	10.3
A2	M141	17.4	32.2	21.0	23.5	22.6	22.8	22.6	27.5	16.6	16.6	10.2	26.8	12.3	10.6	10.6
B1	M141	14.2	27.4	17.2	32.3	31.7	3.2	3.1	15.8	12.6	9.7	7.5	20.2	9.7	7.7	7.7
A1B	M217	11.7	16.5	13.8	14.6	14.2	14.2	14.2	40.5	14.5	35.5	10.7	23.7	12.2	9.5	11.0
A2	M217	10.1	15.1	12.5	13.8	13.5	13.5	13.5	49.0	16.2	32.5	12.5	26.2	13.9	12.0	13.0
B1	M217	8.3	13.3	10.3	19.1	18.9	1.9	1.8	48.8	16.3	30.8	10.7	27.0	13.0	10.4	11.1
A1B	M410	10.9	16.6	13.8	14.7	14.3	14.3	14.3	22.7	16.2	38.4	11.6	26.9	13.4	10.9	12.0
A2	M410	9.5	15.8	12.6	13.9	13.5	13.6	13.5	31.0	16.1	29.7	9.0	27.7	13.1	8.8	9.3
B1	M410	7.8	13.1	10.3	19.2	19.0	1.9	1.8	20.8	12.4	20.9	8.0	21.4	10.2	8.4	8.2
A1B	M424	11.0	13.9	12.6	13.7	13.1	13.1	13.1	51.7	21.8	43.4	14.0	33.0	16.9	13.7	14.5
A2	M424	9.9	11.8	11.5	12.8	12.1	12.2	12.1	54.0	25.3	45.4	18.1	38.7	21.2	18.0	18.9
B1	M424	7.9	11.3	9.5	17.8	17.5	1.6	1.5	45.8	16.6	26.0	10.5	25.3	12.8	10.7	10.8
A1B	M541	13.4	15.2	13.7	14.9	14.3	14.3	14.3	27.4	20.8	24.9	12.0	33.9	14.8	14.0	12.4
A2	M541	12.1	13.4	12.6	14.1	13.4	13.4	13.4	39.1	22.6	24.1	13.7	36.9	16.8	16.0	14.3
B1	M541	9.7	13.2	10.8	20.6	20.2	1.3	1.2	29.5	16.8	18.0	9.7	26.5	12.1	11.0	10.1

SC	Site	Runoff change [%]						
		Min	Q1	Av	Q3	Max	Av RMSE	Av BIAS
A1B	TM	−36.0	−0.4	7.3	9.1	42.8	33.7	7.3
A2	TM	−47.6	−2.1	10.0	13.0	64.4	38.5	8.9
B1	TM	−32.9	1.2	8.3	10.2	39.1	32.6	8.2
A1B	MS	−37.1	3.5	11.4	13.7	33.0	32.1	11.0
A2	MS	−48.4	1.3	11.5	14.5	41.3	34.9	10.3
B1	MS	−39.4	1.4	7.1	8.5	22.7	28.2	7.1

HESSD
10, 6445–6471, 2013

Table 3. VHM model performance evaluation for calibration and validation period after different calibration methods.

Calibration Method Evaluation	Tomebamba in Monay (1260 km^2) Step Wise	Optimized Step-Wise	Optimized Overall	Matadero in Sayausi (300 km^2) Step Wise	Optimized Step-Wise	Optimized Overall
NS eff Ob	0.689	0.688	0.689	0.699	0.640	0.681
NS eff BF	0.701	0.688	−0.383	0.655	0.449	0.428
NS eff IF	0.577	0.554	−0.349	0.605	0.601	0.114
NS eff OF	0.405	0.385	−3.066	0.485	0.480	−0.688
H Pk E [mm.d^{-1}.km^2]	1.148	1.184	1.221	0.389	0.505	0.463
L Pk E [mm.d^{-1}.km^2]	0.172	0.152	2.976	0.253	0.239	0.534

HESSD
10, 6445–6471, 2013

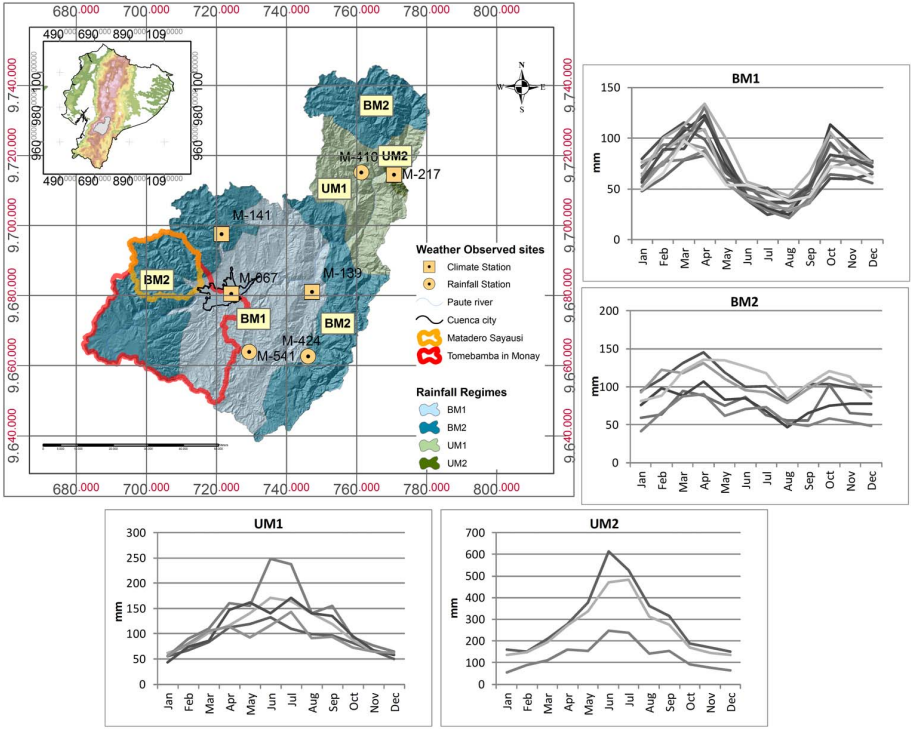

Fig. 1. Rainfall regimes in the Paute river basin (BM1, BM2, UM1 and UM2): spatial regions (left), monthly rainfall depths for different observation sites in each region.

HESSD
10, 6445–6471, 2013

Climate changes of hydrometeorological and hydrological extremes

D. E. Mora et al.

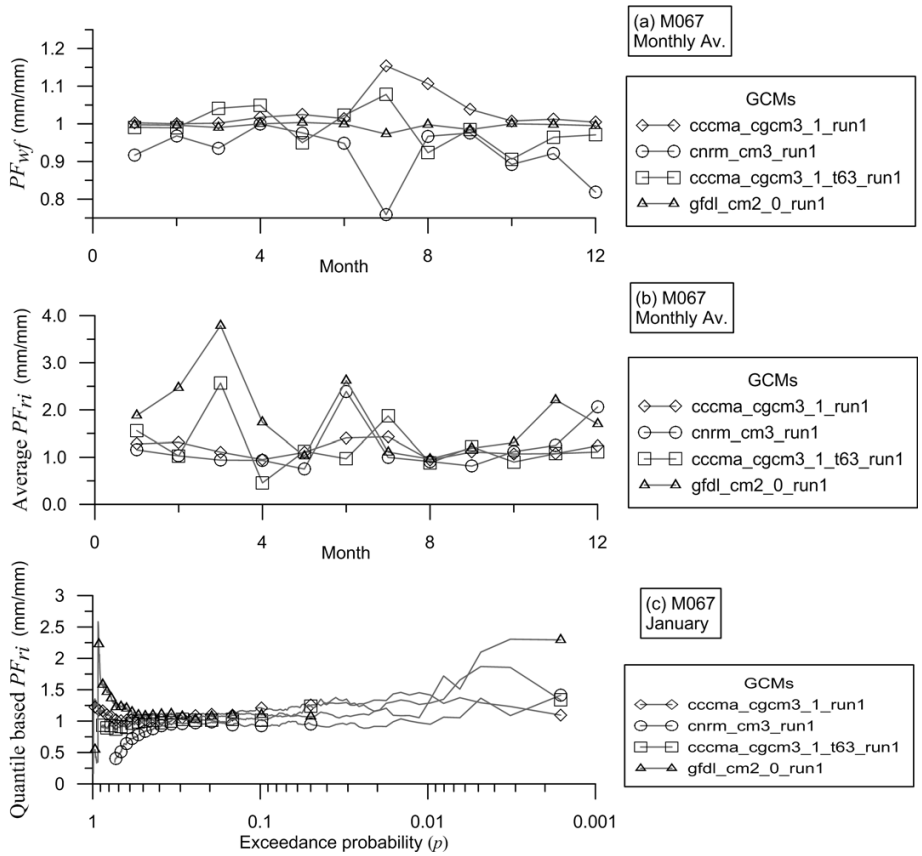

Fig. 2. (a) Perturbation factor of the wet day frequency PF_{wf}, **(b)** perturbation factor of the rainfall intensity PF_{ri} averaged for each month and **(c)** quantile based PF_{ri} for January in site M067 for the four selected GCM runs.

HESSD
10, 6445–6471, 2013

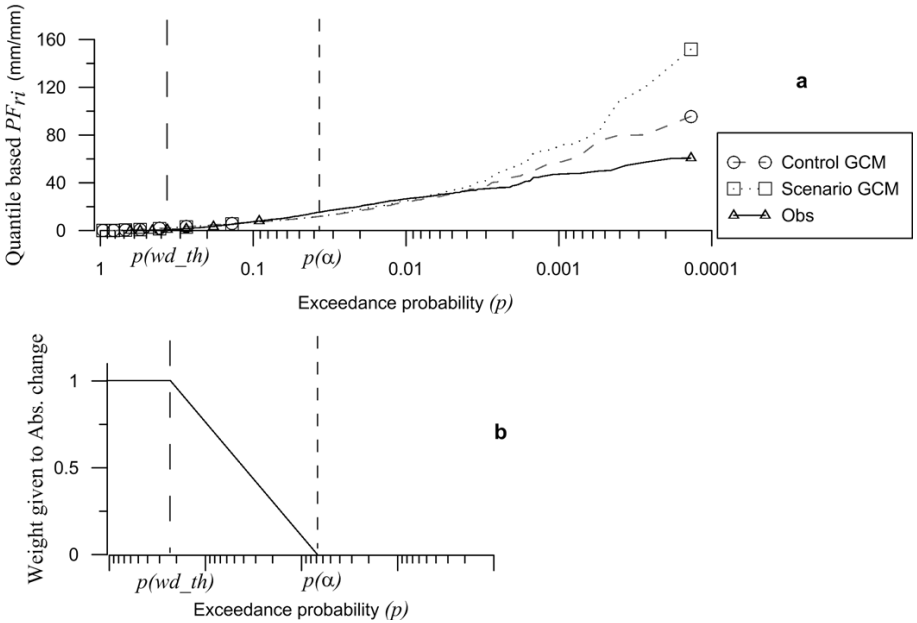

Fig. 3. (a) Illustration of the second adjustment to the QPA including an exceedance probability threshold value $p(\alpha)$ for site M067 and GCM run cnrm_cm3_run1; **(b)** relative weight given to absolute change (vs. relative change).

HESSD
10, 6445–6471, 2013

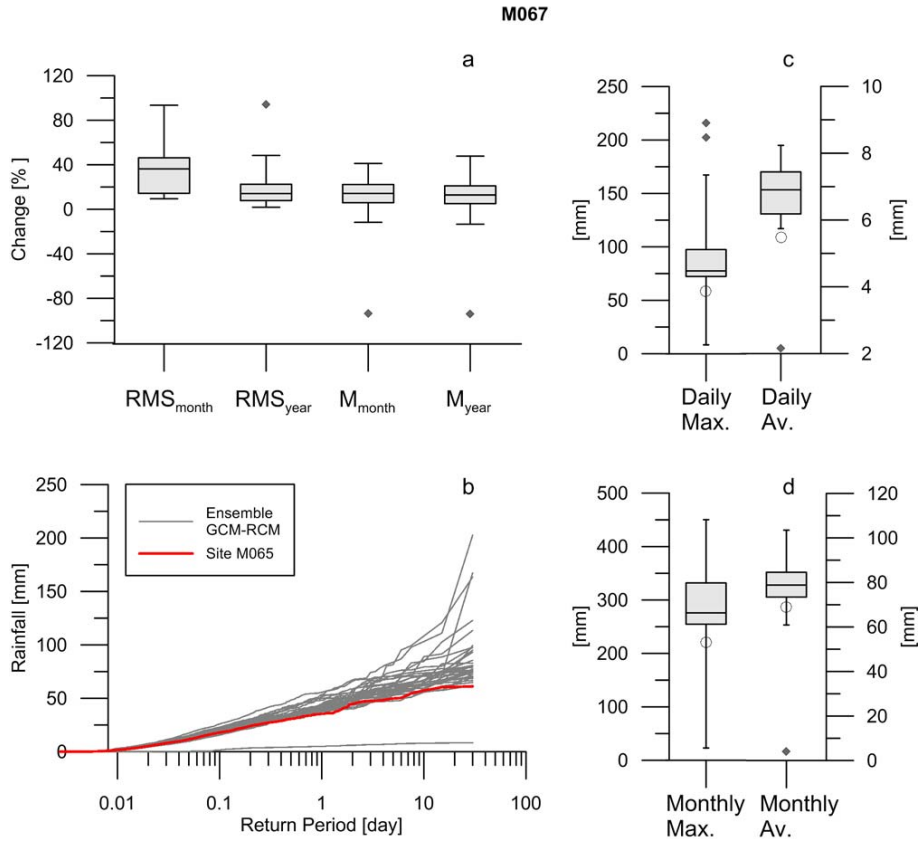

Fig. 4. Rainfall results of the ensemble perturbed observed series for all climate models for site M067 and scenario A1B according to the impact indicators: **(a)** monthly and yearly root mean square and mean change, **(b)** rainfall extremes vs return period, **(c)** daily maxima and average rainfall, **(d)** monthly maxima and average rainfall. Outlier values are shown as dark dots. Observed values are shown as blank circles.

HESSD
10, 6445–6471, 2013

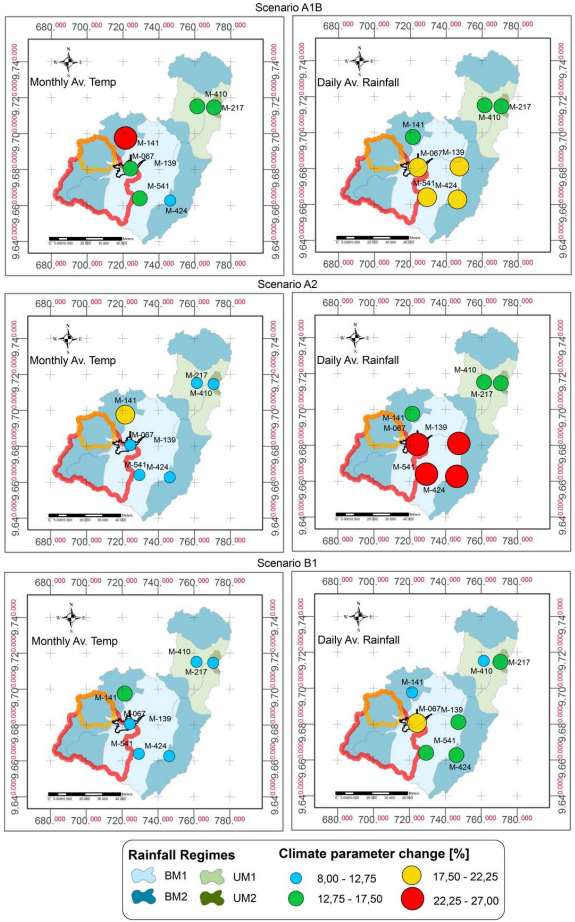

Fig. 5. Maps of change [%] on the average monthly mean temperature and the average daily rainfall after downscaling for seven sites in the Paute River Basin under influence of different climate change signals and scenario SRES A1B, A2 and B1.

HESSD
10, 6445–6471, 2013

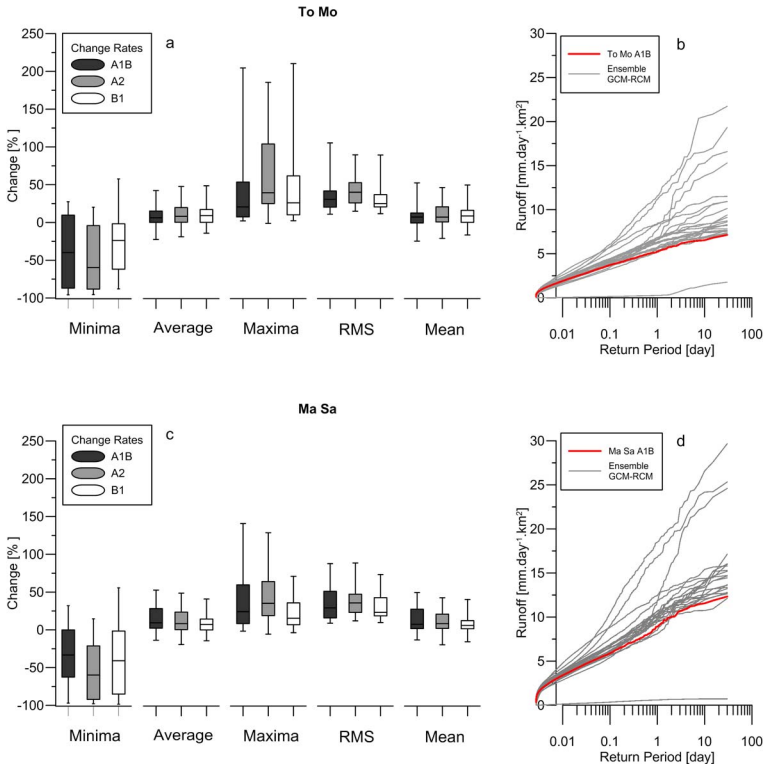

Fig. 6. Results of changes in daily runoff: **(a)** percentage changes on the minima, average, maxima, RMS and mean runoff for To Mo catchment, **(b)** extreme runoff versus empirical return period for To Mo catchment, **(c)** percentage changes on the minima, average, maxima, RMS and mean runoff for Ma Sa catchment, **(d)** extreme runoff versus empirical return period for Ma Sa catchment; b and d for scenario A1B.

HESSD
10, 6445–6471, 2013